Fracture toughness, hardness, and Young's modulus of tantalum nanocrystalline films

G. Guisbiers, E. Herth, L. Buchaillot, T. Pardoen

Fracture toughness, hardness, and Young's modulus of tantalum nanocrystalline films

Cite as: Appl. Phys. Lett. **97**, 143115 (2010); https://doi.org/10.1063/1.3496000
Submitted: 26 July 2010 • Accepted: 10 September 2010 • Published Online: 07 October 2010

G. Guisbiers, E. Herth, L. Buchaillot, et al.

Fracture toughness, hardness, and Young's modulus of tantalum nanocrystalline films

G. Guisbiers,[1,a)] E. Herth,[2] L. Buchaillot,[2] and T. Pardoen[1]
[1]*Institute of Mechanics, Materials, and Civil Engineering, UCL, Place Sainte Barbe 2, B-1348 Louvain-la-Neuve, Belgium*
[2]*CNRS-UMR8520, IEMN, Scientific City, Avenue Henri Poincaré BP60069, F-59652 Villeneuve d'Ascq, France*

(Received 26 July 2010; accepted 10 September 2010; published online 7 October 2010)

The fracture toughness, hardness, and Young's modulus of tantalum thin films are investigated based on nanoindentation measurements. A lower estimate of the fracture toughness of a 100 nm tantalum film is 0.28 ± 0.07 MPa $m^{1/2}$. The hardness increases when reducing the film thickness whereas Young's modulus decreases slightly. More precisely, the hardness of the 100 nm thick film is four times higher than the bulk behavior. A simple theoretical model, based on the connection between Young's modulus and melting temperature, predicts an inverse grain size variation in Young's modulus confirmed by experiments. © *2010 American Institute of Physics*.
[doi:10.1063/1.3496000]

Despite the huge amount of literature dedicated to the size dependency of mechanical properties,[1–3] the fracture behavior of nanocrystalline materials is still not well understood due to many factors influencing it.[4,5] Moreover, the yield strength and hardness exhibit a Hall–Petch behavior or an inverse one depending on the nanograin size.[6] Additionally, Young's modulus varies also with size.[7] A common point to all these size-dependent mechanical properties is the important role played in nanocrystalline materials by the large amount of grain boundaries which are places where interatomic bonds are weak compared to bulk.[4] In the present study, elastic, plastic, and fracture properties of tantalum nanocrystalline films are investigated by nanoindentation as tantalum is used in many technological applications such as diffusion barrier in nano/microelectronics and wear protection coatings.[8]

Tantalum thin films were deposited on silicon substrate by e-beam evaporation.[9,10] The curvature of the system was measured using a profilometer (DEKTAK 3030 from Veeco) in order to extract the residual stress. The films were characterized by a scanning electronic microscope (SEM, Ultra 55 from Zeiss), an atomic force microscope (AFM, Nanoscope IIIa from Veeco), and a nanoindenter (XP from MTS).

The hardness and Young's modulus are extracted from the load-indentation depth data using the Oliver and Pharr method.[11,12] The hardness is defined by $H=P_{\max}/A_p$, where $P_{\max}$ is the peak indentation load and A_p is the projected area of the hardness impression. Young's modulus is defined by $E=(1-\nu^2)[\sqrt{A_p/\pi}2\beta/S-(1-\nu_i^2)/E_i]^{-1}$, where ν is the Poisson ratio and E_i and ν_i are the same parameters for the indenter tip material. The stiffness, S, is obtained from the tangent of the unloading part at the peak indentation load in the load-displacement curve. For a Berkovitch indenter (three sided pyramid), $\beta=1.034$, $A_p=3\sqrt{3}h_f^2 \tan^2\theta$, where h_f is the final depth of the contact impression after unloading and $\theta=65.27°$ is the face angle with respect to the central axis of the indenter.[12] The usual indentation size effect (i.e., hardness increases with a decreasing indentation depth) is observed for indents with a depth to thickness ratio, δ, of up to ~0.2.[13] The substrate effect (i.e., hardness increases with an increasing indentation depth) occurs when δ is above ~0.75 (Ref. 14) for the elastic modulus mismatch in the present system. Therefore, the indentation depth range was chosen in such a way that H and E are almost constant with δ, i.e., between 50–70 nm for the 100 nm film and 60–90 nm for 200 nm film (inset of Fig. 1). For each film, 15 indentations were made and only the average value is indicated in Table I.

In polycrystalline materials, it is well known that the grain boundary strengthening is described by the Hall–Petch relation,[15,16] i.e., the yield strength of the material increases when the grain size decreases as follows: $\sigma_y(D)=\sigma_{y,\infty}+k_{y_1}D^{-1/2}$, where $\sigma_y(D)$ is the size-dependent yield strength, $\sigma_{y,\infty}$ is the bulk yield strength, k_{y_1} is the strengthening coefficient, and D is the grain size, measured on the AFM images

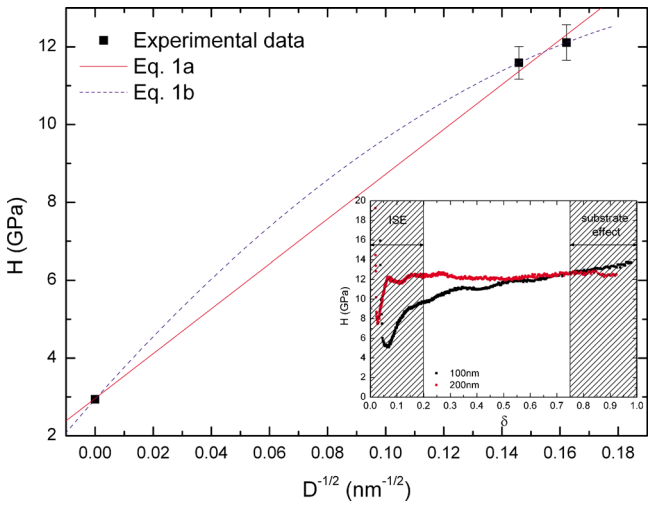

FIG. 1. (Color online) Hardness vs the inverse square root of the grain size. The linear and parabolic fits are indicated with solid and dashed lines, respectively. Inset: Hardness vs the indentation depth to thickness ratio for 100 and 200 nm films. The zones, where the indentation size effect and the substrate effect occur, are indicated.

a)Author to whom correspondence should be addressed. Electronic mail: gregory.guisbiers@physics.org. Tel.: 003210473059. FAX: 003210474028.

TABLE I. Properties of tantalum thin films measured by profilometry, microscopy, and nanoindentation.

Thickness (nm)	σ (MPa)	rms (nm)	Grain size (nm)	E (GPa)	H (GPa)	p (%)
100	641 ± 156	1.1	38 ± 1	176.1 ± 3.6	12.11 ± 0.46	10 ± 2
200	351 ± 104	1.8	47 ± 1	175.0 ± 3.4	11.59 ± 0.42	12 ± 2
400	159 ± 21	13.4	47 ± 1	Not measurable		21 ± 2
600	88 ± 23	31.6	36 ± 1	Not measurable		83 ± 8
Bulk	/	/	/	185[a]	2.94[a]	/

[a]Reference 33.

by the power spectral density.[17] For nanocrystalline materials, an inverse relationship $\sigma_y(D)=\sigma_{y,\infty}+k_{y_2}D^{-1}$ can be justified as the size of dislocation source scales proportional to the grain size.[18] Hardness follows also the Hall–Petch relation due to its proportionality to yield strength, $H \sim 3\sigma_y$ for metals,[19]

$$H(D) = H_\infty + k_{H_1} D^{-1/2}, \tag{1a}$$

$$H(D) = H_\infty + k_{H_2} D^{-1/2} + k_{H_3} D^{-1}, \tag{1b}$$

where $H(D)$ is the size-dependent hardness of the material, H_∞ is the bulk hardness, k_{H_1} is the slope in the size-dependent hardness versus $D^{-1/2}$ (Fig. 1); and k_{H_2} and k_{H_3} are the coefficients of a parabolic relationship between hardness and $D^{-1/2}$. The resulting k_{H_1}, k_{H_2}, and k_{H_3} values have been determined to be equal to 58 ± 4 GPa $\text{nm}^{1/2}$, 84 ± 1 GPa $\text{nm}^{1/2}$, and -170 ± 1 GPa nm, respectively. The very high hardness of Ta nanocrystalline films has already been reported by Zhang *et al.*[20] for rf magnetron sputtered layers. They measured a hardness value equal to 11.6 ± 0.4 GPa for films with an average grain size of 76.5 nm which is quite close to our value of 12.1 ± 0.5 GPa for a 38 nm grain size, even though the deposition process is different. Zhang *et al.*[20] have announced that the highest hardness should be attained with a grain size equal to 35 nm which is close to the present data.

Different trends have been reported in the literature regarding the dependence of Young's modulus with size.[5,21] Ao *et al.*[7] have explained this behavior due to the competition between the surface bond shrinkage and melting temperature variation with size reduction. According to Gu *et al.*,[22] the size-dependent Young's modulus of the material, $E(D)$, can be related to its Debye temperature $T_{\text{Debye}}(D)$, knowing the corresponding bulk quantities, $E(D)/E_\infty = [T_{\text{Debye}}(D)/T_{\text{Debye},\infty}]^2$. It has been shown previously[23,24] that the size-dependent behavior of the Debye temperature and melting temperature are related and can be expressed by $T_m(D)/T_{m,\infty} = [T_{\text{Debye}}(D)/T_{\text{Debye},\infty}]^2 = 1 - \alpha_{\text{shape}}/D$, where $T_m(D)$ is the melting temperature and α_{shape} is the parameter quantifying the size effect on the material property, depending on the shape of the nanostructure. This parameter is defined as $\alpha_{\text{shape}} = [D(\gamma_s - \gamma_l)\Delta H_{m,\infty}/](A/V)$, where A/V is the surface area over volume ratio, $\Delta H_{m,\infty}$ is the bulk melting enthalpy, and $\gamma_{s(l)}$ the surface energy in the solid (liquid) phase. Therefore, the following size dependence of Young's modulus is proposed as follows:

$$E(D)/E_\infty = 1 - \alpha_{\text{shape}}/D. \tag{2}$$

This relationship agrees with our experiments and literature data from Ref. 25 (Fig. 2). Zhang *et al.*[20] obtained 178 GPa for films with an average grain size equal to 76.5 nm while the present results give 176.1 ± 3.6 GPa for a 38 nm grain size. Note that this apparent elastic softening could also be due to an increasing porosity in thinner films.[25,26] The open porosity, p, which refers to the fraction of total volume in which a fluid flow can effectively take place (i.e., it excludes closed pores) has been measured by AFM (Ref. 27) while the closed porosity could not be measured. As indicated by Table I, the open porosity increases with film thickness and thus cannot explain the decreasing behavior of Young's modulus. Nevertheless, it can be shown theoretically that the closed porosity plays a role in the decreasing behavior of Young's modulus as the grain boundary energy is lower than the surface energy ($\gamma_{GB} < \gamma_s$), therefore coalescence of nanograins reduces the value of α_{shape} and then decreases the size effect on Young's modulus.

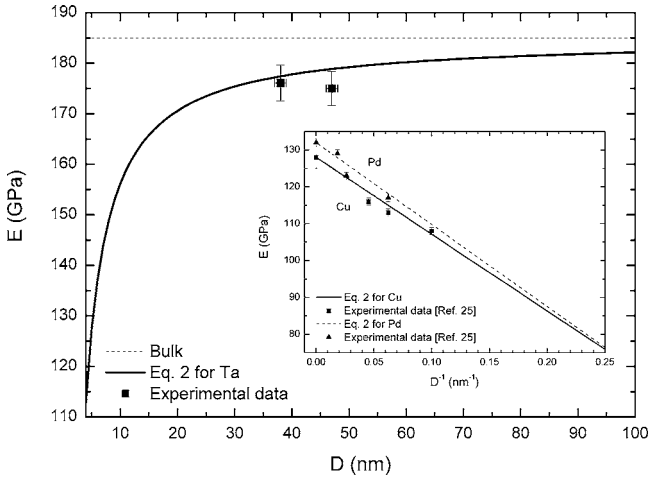

FIG. 2. Young's modulus vs the grain size [$\alpha_{\text{shape}}(\text{Ta}) = 1.56$ nm, see Ref. 34]. The inset indicates Young's modulus behavior vs the inverse grain size for Pd and Cu [$\alpha_{\text{shape}}(\text{Pd}) = 1.68$ nm and $\alpha_{\text{shape}}(\text{Cu}) = 1.63$ nm, see Ref. 34]. The experimental data for Pd and Cu are taken from Ref. 25.

Scanning probe microscopy characterization (SEM and AFM) shows that the 100 and 200 nm thick films do not contain cracks while the 400 and 600 nm thick films exhibit a dense crack pattern. More precisely, the 400 nm film [Fig. 3(a)] is cracked but sticks to the silicon substrate whereas the 600 nm film is completely delaminated [Fig. 3(b)]. Discontinuities are observed in the load-displacement curves; 100 and 200 nm thick films exhibit a step in the unloading part of the load-displacement curve (called "pop-out"[19]) while 400 and 600 nm thick films have a step in the loading part of the load-displacement curve (called "pop-in"[19]). This observation shows that the 400 and 600 nm thick films are cracked before indentation while the 100 and 200 nm thick films crack during indentation. Indeed, the competition between strain energy minimization and surface energy minimization controls the cracking of the films.[28] The strain energy minimization is favored in thicker films whereas surface energy minimization is favored in thinner films. The tendency for relaxation by cracking increases with increasing thickness as the energy release rate scales proportionally to the thickness[29] whereas thinner films can relax more easily by diffusion along grain boundaries. The energy release rate of an isolated crack which is long compared to the thickness of the film G is proportional to the thickness as indicated by $G = 1.98\sigma^2 t/E$,[29] where t is the thickness of the film; σ being the stress in the film at a remote distance from the crack. The

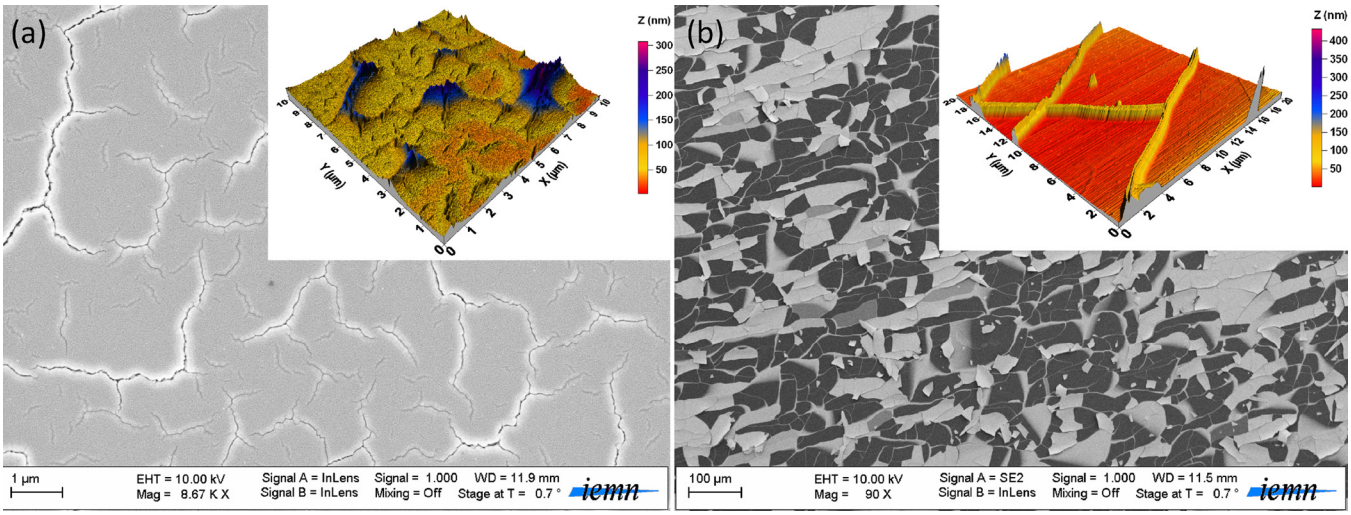

FIG. 3. (Color online) (a) SEM image of a Ta film with a thickness equal to 400 nm. Inset: AFM image of the Ta film with a thickness equal to 400 nm. (b) SEM image of the Ta film with a thickness equal to 600 nm. Inset: AFM image of the Ta film with a thickness equal to 600 nm. These observations are made before indentation.

crack propagates if G is higher than a critical value, G_c. The stress was evaluated through the measurement of the curvature of the film-substrate system, κ, by using Stoney's equation,[30] i.e., $\sigma=\kappa E_s t_s^2/[6(1-\nu_s)t]$, where E_s and ν_s are Young's modulus and Poisson ratio of the substrate, respectively, and t_s is the thickness of the substrate. Stoney's equation is still valid as long as the ratio t/t_s is smaller or equal to 0.1.[31] As shown in Table I, the residual stress state in the Ta films is tensile and decreases when the thickness increases, illustrating the existence of a relaxation process. For the 100 and 200 nm thick films, a lower limit on the critical energy release rate could be estimated as $G_c=0.46\pm0.20$ J/m^2 and $G_c=0.28\pm0.19$ J/m^2, respectively, using the measured residual stress σ. The stress intensity factor is related to the energy release rate by $K_{IC}=\sqrt{EG_c}$ assuming plane stress conditions.[5] The corresponding lower bound for the stress intensity factor for the 100 and 200 nm thick films are $K_{IC}=0.28\pm0.07$ MPa m$^{1/2}$ and $K_{IC}=0.22\pm0.06$ MPa m$^{1/2}$, respectively. These values can be compared with $K_{IC}=0.78$ MPa m$^{1/2}$, the value announced by Gruber *et al.*[32] for the bilayer system; Ta-19 nm-Cu-71 nm. They have shown that for a constant copper thickness, K_{IC} decreases by increasing the thickness of the Ta film.

As a conclusion, a lower limit on the critical energy release rate for cracking has been determined for Ta nanocrystalline films. As expected, hardness follows the Hall–Petch relation for the investigated thickness range and an inverse grain size dependency of Young's modulus is observed. A theoretical equation has been deduced from thermodynamics to evaluate the size-dependency of Young's modulus and was found to be in agreement with experimental data.

G. Guisbiers would like to thank the Belgian Federal Science Policy Office (BELSPO) through the "Mandats de retour" action for their financial support. The support of BELSPO for the Belgian Interuniversity Attraction Pole (IAP) P6/24 is gratefully acknowledged.

[1]M. A. Meyers, A. Mishra, and D. J. Benson, Prog. Mater. Sci. **51**, 427 (2006).
[2]N. M. Jennett, R. Ghisleni, and J. Michler, Appl. Phys. Lett. **95**, 123102 (2009).
[3]W. W. Gerberich, J. Michler, W. M. Mook, R. Ghisleni, F. Ostlund, D. D. Stauffer, and R. Ballarini, J. Mater. Res. **24**, 898 (2009).
[4]I. A. Ovid'ko, J. Mater. Sci. **42**, 1694 (2007).
[5]W. W. Gerberich, W. M. Mook, M. J. Cordill, J. M. Jungk, B. Boyce, T. Friedmann, N. R. Moody, and D. Yang, Int. J. Fract. **138**, 75 (2006).
[6]C. S. Pande and K. P. Cooper, Prog. Mater. Sci. **54**, 689 (2009).
[7]Z. M. Ao, S. Li, and Q. Jiang, Appl. Phys. Lett. **93**, 081905 (2008).
[8]D. Kaufmann, R. Mönig, C. A. Volkert, and O. Kraft, "Size dependent mechanical behaviour of tantalum," Int. J. Plast. (to be published).
[9]G. Guisbiers, S. Strehle, and M. Wautelet, Microelectron. Eng. **82**, 665 (2005).
[10]G. Guisbiers, S. Strehle, O. Van Overschelde, and M. Wautelet, AIP Conf. Proc. **817**, 317 (2006).
[11]W. C. Oliver and G. M. Pharr, J. Mater. Res. **7**, 1564 (1992).
[12]A. C. Fisher-Cripps, *Nanoindentation*, 2nd ed. (Springer, New York, 2004).
[13]Y. Cao, S. Allameh, D. Nankivil, S. Sethiaraj, T. Otiti, and W. Soboyejo, Mater. Sci. Eng., A **427**, 232 (2006).
[14]R. Saha and W. D. Nix, Acta Mater. **50**, 23 (2002).
[15]E. O. Hall, Proc. Phys. Soc. London, Sect. B **64**, 747 (1951).
[16]N. J. Petch, J. Iron Steel Inst. **174**, 25 (1953).
[17]G. Guisbiers, O. Van Overschelde, M. Wautelet, P. Leclere, and R. Lazzaroni, J. Phys. D: Appl. Phys. **40**, 1077 (2007).
[18]M. Zhao, J. C. Li, and Q. Jiang, J. Alloys Compd. **361**, 160 (2003).
[19]B. Bhushan, *Handbook of Nanotechnology*, 2nd ed. (Springer, New York, 2006).
[20]M. Zhang, B. Yang, J. Chu, and T. G. Nieh, Scr. Mater. **54**, 1227 (2006).
[21]X. J. Liu, J. W. Li, Z. F. Zhou, L. W. Yang, Z. S. Ma, G. F. Xie, Y. Pan, and C. Q. Sun, Appl. Phys. Lett. **94**, 131902 (2009).
[22]M. X. Gu, C. Q. Sun, Z. Chen, T. C. Au Yeung, S. Li, C. M. Tan, and V. Nosik, Phys. Rev. B **75**, 125403 (2007).
[23]G. Guisbiers and L. Buchaillot, Phys. Lett. A **374**, 305 (2009).
[24]G. Guisbiers, Nanoscale Res. Lett. **5**, 1132 (2010).
[25]P. G. Sanders, J. A. Eastman, and J. R. Weertman, Acta Mater. **45**, 4019 (1997).
[26]J. Kováčik, J. Mater. Sci. Lett. **18**, 1007 (1999).
[27]I. Horcas, R. Fernández, J. M. Gómez-Rodríguez, J. Colchero, J. Gómez-Herrero, and A. M. Baro, Rev. Sci. Instrum. **78**, 013705 (2007).
[28]C. V. Thompson and R. Carel, J. Mech. Phys. Solids **44**, 657 (1996).
[29]F. Delannay and P. Warren, Acta Metall. Mater. **39**, 1061 (1991).
[30]G. G. Stoney, Proc. R. Soc. London, Ser. A **82**, 172 (1909).
[31]C. A. Klein, J. Appl. Phys. **88**, 5487 (2000).
[32]P. A. Gruber, E. Arzt, and R. Spolenak, J. Mater. Res. **24**, 1906 (2009).
[33]W. Martienssen and H. Warlimont, *Springer Handbook of Condensed Matter and Materials Data* (Springer, Berlin, 2005).
[34]G. Guisbiers, M. Kazan, O. Van Overschelde, M. Wautelet, and S. Pereira, J. Phys. Chem. C **112**, 4097 (2008).